A Priori Prediction of Heats of Vaporization and Sublimation by EFP2-MD

ARTICLE *in* THE JOURNAL OF PHYSICAL CHEMISTRY B · APRIL 2014

Impact Factor: 3.3 · DOI: 10.1021/jp500365z · Source: PubMed

3 AUTHORS:

Manik Ghosh
University of Limerick
26 PUBLICATIONS **167** CITATIONS
SEE PROFILE

Soo Gyeong Cho
Agency for Defense Development
60 PUBLICATIONS **360** CITATIONS
SEE PROFILE

Cheol Ho Choi
Kyungpook National University
111 PUBLICATIONS **2,123** CITATIONS
SEE PROFILE

THE JOURNAL OF PHYSICAL CHEMISTRY B

Article

pubs.acs.org/JPCB

A Priori Prediction of Heats of Vaporization and Sublimation by EFP2-MD

Manik Kumer Ghosh,[†] Soo Gyeong Cho,[‡] and Cheol Ho Choi*,[†]

[†]Department of Chemistry and Green-Nano Materials Research Center, College of Natural Sciences, Kyungpook National University, Sangyeok, Bukgu, Daegu 702-701, South Korea

[‡]Defense Advanced R&D Institute, Agency for Defense Development (ADD), Daejeon, South Korea

ABSTRACT: New theoretical procedures were proposed for the heats of vaporization (ΔH_{vap}) and sublimation (ΔH_{sub}) predictions by adopting effective fragment potential version 2—molecular dynamics (EFP2-MD) simulations. The particular EFP2, as generated by HF/6-31++G(2d,2p), yielded excellent results in the predictions of ΔH_{vap}, where mean absolute deviation (MAD) and root-mean-square deviation (RMSD) for 16 molecules were 0.34 and 0.44 kcal/mol, respectively. By introducing a uniform scaling factor, we further derived a prediction procedure for ΔH_{sub}, where its MAD and RMSD were 0.76 and 0.90 kcal/mol, respectively. Because EFP2-MD does not require any ab initio computations during simulation, computational overhead of our procedures is minimal. We believe that our new procedures for the ΔH_{vap} and ΔH_{sub} predictions could be widely applicable in the areas where accurate chemical information for virtual molecules is critical.

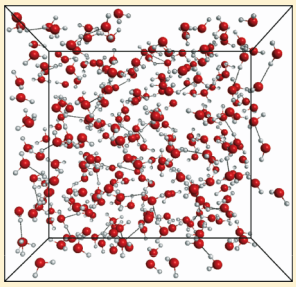

I. INTRODUCTION

In designing new materials, accurate prediction of various thermochemical properties is of significant importance to obtain the final properties that the researchers want to estimate. The heat of formation is one of the most important properties, which provides useful pieces of information regarding internal energy, chemical stability, and reaction rate. In some cases, particularly in high-energy molecules (HEMs), molecular designing programs require heat of formation in condensed phases as input information. For example, most of programs for the predictions of explosive performance including CHEETAH[1] and EXPLO-5[2] require heats of formation of all ingredients in their most stable phase under the ambient condition. Most of the HEMs are solid or liquid phases under the ambient condition, requiring additional enthalpy change data of phase transition.

Because experimental heats of formation in condensed phase are not usually available, researchers often turn their attention to ab initio calculations to predict the explosive performance for those molecules. Because of the fact that ab initio calculations are limited to the thermochemical properties only for the gas phase, additional procedures are needed for the thermochemical predictions of phase changes such as heats of vaporization (ΔH_{vap}) and sublimation (ΔH_{sub}) to obtain condensed phase properties. However, a priori prediction of thermochemical properties of phase changes is a daunting task. Most of the previous studies proposed knowledge-based methods. In this approach, the value of a property of interest for a compound was predicted based on empirically determinable contributions from the structural fragments.[3] Dalmazzone et al.[4] also proposed another group additivity method for the prediction of critical temperatures and enthalpies of vaporization of covalent compounds. Politzer et al.[5] proposed a method for the predictions of heats of vaporization and sublimation, which is based on the calculated electrostatic potential on the molecular surface.

ΔH_{vap} is defined as the enthalpy change in the conversion of one mole of liquid to a gas at constant temperature. In experiments, the heat of vaporization can be measured at the boiling point of the neat liquid through calorimetry or determined from the vapor pressure—temperature (P—T) plot using the Clausius—Clapeyron equation. Theoretically, ΔH_{vap} can be calculated as[6]

$$\Delta H_{vap}(T) = H(p, T)_{gas} - H(p, T)_{liquid} = E(T)_{gas} - E(T)_{liquid} + p(V_{gas} - V_{liquid}) \quad (1)$$

where $H(p,T)_{gas}$ and $H(p,T)_{liquid}$ are the enthalpies in the gas and liquid phases, respectively. $E(T)_{gas}$ and $E(T)_{liquid}$ are the total energies of the gas and liquid phases, respectively.

With the assumptions that (1) the V_{liquid} is negligible compared with V_{gas}, (2) a molecule behaves ideally ($pV_{gas} = RT$), (3) the kinetic energies of a molecule in the gas and liquid phases are identical at the same temperature, (4) the intramolecular energy in the liquid phase is the same as that in the gas phase, and (5) all internal degrees of freedom of individual molecules are frozen in the liquid phase, eq 1, can be significantly simplified to

$$\Delta H_{vap}(T) = E(T)_{liquid}^{inter\text{-}pot} + RT \quad (2)$$

where $E(T)_{liquid}^{inter\text{-}pot}$ is the intermolecular potential energy in the liquid phase.

Received: January 13, 2014
Revised: April 8, 2014
Published: April 10, 2014

Consequently, ΔH_{vap} is almost exclusively associated with the nonbonded interactions, which are composed of van der Waals and electrostatic contributions.[7] The intermolecular potential energy in eq 2 can be readily obtained by molecular dynamics (MD) simulations. However, classical MD simulations are performed on the basis of empirical force fields, which were parametrized using both ab initio and high-quality experimental data. Molecular mechanical force fields purely based on ab initio calculations usually do not have a satisfactory performance in predicating the molecular properties of liquid or solid phases. Therefore, successful development of accurate empirical force fields requires the availability of experimental thermodynamic data such as ΔH_{vap} for small molecules. Therefore, completely new parametrization schemes would be desirable, which would ultimately provide a way for a priori predictions of these intermolecular equilibrium properties, to overcome the experimental dependencies. As a first step toward the goal, the applicability of the fully ab initio driven effective fragment potential (EFP)[8] for the ΔH_{vap} predictions was investigated in this paper.

Gordon and coworkers[8] have been developing a purely theoretical EFP, which was originally developed specifically to describe intermolecular interactions. In particular, the version 2 of EFP (EFP2) included all of the essential physics and had no empirically fitted parameters. The EFP is composed of Coulomb, polarization, exchange-repulsion, dispersion, and charge-transfer terms. Coulomb term refers to the Coulomb portion of the electrostatic interaction up to octopoles. Polarization term is the induction or polarization part of the electrostatic interaction. This term is represented by the interaction of the induced dipole on one fragment with the permanent dipole on another fragment, expressed in terms of the dipole polarizability. This dipole-induced dipole term is iterated to self-consistency, so many body effects are included. The quantum-mechanical exchange repulsion term is derived as an expansion in the intermolecular overlap. The dispersion interaction is expressed in terms of localized molecular orbital (LMO)−LMO interactions. The charge-transfer interaction is derived by considering the interactions between the occupied valence molecular orbitals on one fragment with the virtual orbitals on another fragment. Because the method involves no empirically fitted parameters, an EFP2 for any system can be generated by a "makefp" run in the GAMESS[9] suite of programs. Further descriptions of EFP and references can be found in the recent paper by Gordon et al.[10]

According to our recent attempts of the hybrid QM/EFP-MD,[11] EFP allowed more realistic quantum-mechanical MD simulations (in terms of simulation time and system size) with sufficient accuracy than other methods such as CPMD.[12] The QM/EFP-MD has been successfully utilized in various solution dynamics.[13−16] For our current study, MD simulations with pure EFP2 were mainly adopted for the a priori and accurate predictions of ΔH_{vap}. We have chosen 16 molecules to test our scheme because they were not previously well-predicted by classical MD techniques.[6]

ΔH_{sub} is a simple sum of ΔH_{vap} and heat of fusion (ΔH_{fus}). The direct prediction of ΔH_{fus} is quite complex because it requires a clear understanding of solid-phase structure. Therefore, we introduced a fitting procedure for ΔH_{sub} on the basis of predicted ΔH_{vap}. The detailed procedure shall be explained in the Results and Discussion.

II. COMPUTATIONAL DETAILS

The EFP2 parameters of a given molecule can be generated by a "makefp" run in GAMESS with the options of basis set. We chose three different HF/6-31++G(2d,2p), HF/6-311+G-(2d,2p), and HF/6-311++G(3df,2p) theories for the EFP2 parameter generations to study the basis set effects on the performance of the EFP2. Two additional water models of the classical TIP5P[17] and RHF-based EFP1 (EFP1/HF) were

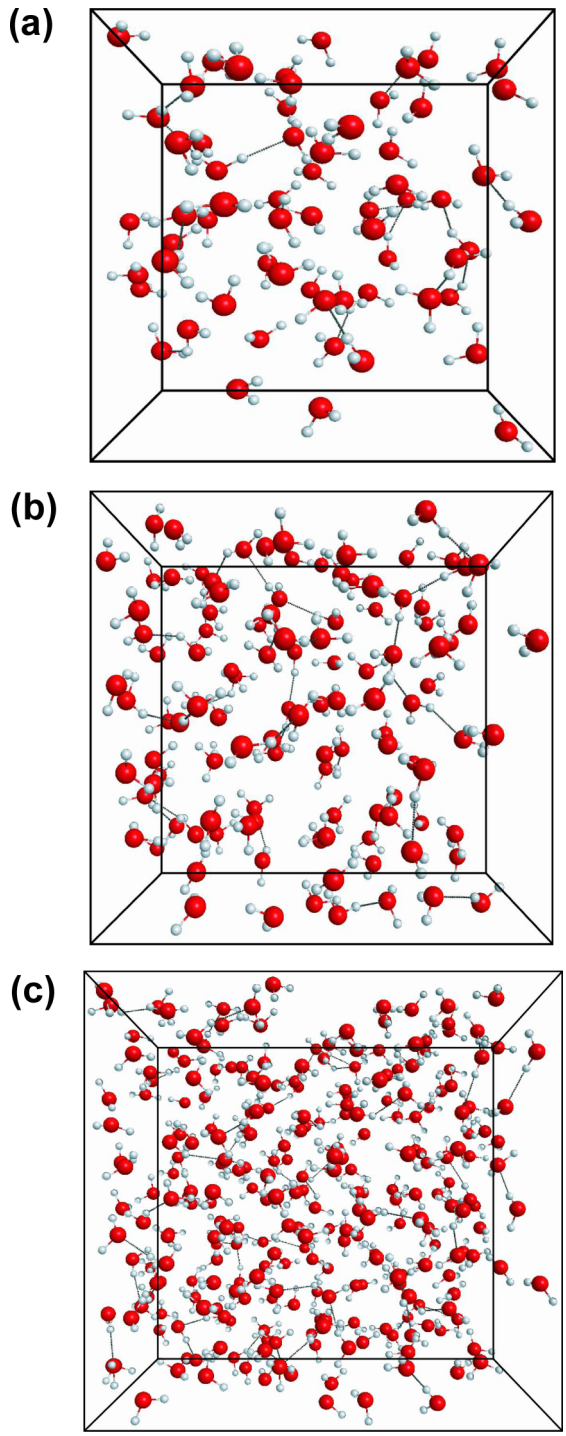

Figure 1. Cubic boxes for the MD simulations with the box lengths of (a) 12.3, (b) 15.0, and (c) 20.0 Å, which constitute 62, 113, and 267 explicit waters, respectively.

dx.doi.org/10.1021/jp500365z | J. Phys. Chem. B 2014, 118, 4876−4882

Table 1. Predicted Heats of Vaporization (ΔH_{vap}) of Water by Canonical MD Simulations[a]

			ΔH_{vap}^{calc}				
					EFP2		
molecule	box length	no. of molecules	TIP5P	EFP1	HF/6-31++G(2d,2p)	HF/6-311+G(2d,2p)	HF/6-311++G(3df,2p)
water	12.3	62	10.38	10.37	11.14	12.85	12.78
	15.0	113	10.40	10.38	11.08	12.77	12.82
	20.0	267	10.37	10.31	11.10	12.69	12.81

[a]Simulations were done with the box lengths of 12.3, 15.0, and 20.0 Å, which constitute 62, 113, and 267 explicit waters, respectively. The values are in kilocalories per mole

Table 2. Predicted Heats of Vaporization (ΔH_{vap}) of 16 Molecules by Canonical MD Simulations[a]

					ΔH_{vap}^{calc}			
						EFP2-MD		
molecule	density	box length	T	ΔH_{vap}^{exp}	AMBER[b]	HF/6-31++G(2d,2p)	HF/6-311+G(2d,2p)	HF/6-311++G(3df,2p)
water	0.997	12.30	25	10.51[c]	10.76 (+0.25)	11.13 (+0.62)	12.85 (+2.34)	12.78 (+2.27)
ethane	0.544	17.85	−88.63	3.51[d]	3.31 (−0.20)	3.60 (+0.09)	3.63 (+0.12)	3.85 (+0.34)
methylamine	0.656	16.95	25	5.59[c]	8.78 (+3.19)	5.90 (+0.31)	5.56 (−0.03)	5.57 (−0.02)
methanol	0.790	16.09	25	8.84 ± 0.48[e]	10.76 (+1.92)	8.853 (−0.01)	9.12 (+0.28)	9.30 (+0.46)
acetonitrile	0.786	17.52	25	7.87[c]	7.56 (−0.31)	8.15 (+0.28)	8.44 (+0.57)	9.62 (+1.75)
acetaldehyde	0.788	17.92	25	6.24[f]	7.14 (+0.90)	6.55 (+0.31)	6.98 (+0.74)	9.09 (+2.85)
1,3-butadiene	0.640	20.57	25	4.99[c]	3.97 (−1.02)	4.87 (−0.12)	5.62 (+0.63)	6.08 (+1.09)
acetone	0.791	19.62	25	7.47[d]	8.16 (+0.69)	7.54 (+0.07)	8.54 (+1.07)	9.69 (+2.22)
acetic acid	1.050	18.06	25	12.33[d]	14.63 (+2.30)	13.11 (+0.78)	13.57 (+1.24)	13.61 (+1.28)
propanol	0.800	19.77	25	11.35 ± 0.10[e]	13.94 (+2.59)	11.53 (+0.18)	11.68 (+0.33)	10.68 (−0.67)
2-propanol	0.781	19.93	25	10.85[c]	14.28 (+3.43)	11.25 (+0.40)	11.45 (+0.60)	9.73 (−1.12)
nitromethane	1.137	17.68	25	9.17[d]	12.66 (+3.49)	10.24 (+1.07)	10.54 (+1.37)	14.55 (+5.38)
2-methyl-2-propanol	0.781	21.38	25	11.14[c]	15.15 (+4.01)	11.46 (+0.32)	11.25 (+0.11)	10.57 (−0.57)
benzene	0.877	20.93	25	7.89 ± 0.48[e]	7.59 (−0.30)	8.28 (+0.39)	8.23 (+0.34)	9.39 (+1.50)
cyclohexane	0.779	22.32	25	7.89 ± 0.48[e]	8.60 (+0.71)	8.24 (+0.35)	8.39 (+0.50)	8.33 (+0.44)
morpholine	1.001	20.77	128	8.87[c]	9.66 (+0.79)	9.06 (+0.19)	9.56 (+0.69)	10.37 (+1.50)
MAD					**1.63**	**0.34**	**0.68**	**1.47**
RMSD					**2.09**	**0.44**	**0.89**	**1.94**

[a]ΔH_{vap}, densities, box lengths, and temperatures are in kilocalories per mole, grams per liter, angstroms, and degrees Celsius, respectively. [b]Ref 6. Note that the values by AMBER were obtained with NPT ensemble, which does not require experimental density. [c]Ref 23. [d]Ref 24. [e]Average value of several pieces of experimental data, specially, 10 data points of cyclohexane, 7 for benzene, 6 for methanol, and 8 for propanol. [f]Ref 25.

adopted for comparisons. Canonical MD simulations with periodic boundary conditions (PBCs) were mainly utilized for the calculations of intermolecular potential energies. It should be noted that canonical ensemble simulations require experimental density. The applicability of EFP2 for the prediction of ΔH_{vap} is mainly tested. To study the box size effect of PBC, we prepared cubic boxes of 12.3, 15.0, and 20.0 Å box lengths containing 62, 113, and 267 explicit water molecules, respectively. (See Figure 1 and Table 1.) The box size and the number of waters were carefully chosen to keep the density constant. All models were equilibrated for at least 25 ps before the 50 ps production runs with the simulation time step of 1 fs. Except ethane and morpoline, all canonical ensemble simulations were done at 298 K by adopting a Nosé−Hoover Thermostat.[18,19] The temperatures of −88.63 and 128 °C were used instead for ethane and morpholine, respectively. The same three sets of EFP2 parameters were also generated for all of the other molecules. For the rest of MD simulations of 15 molecules, the simulation box sizes were calibrated to contain 62 explicit molecules, maintaining the correct density as listed at Table 2. All calculations were performed with the most recent version of GAMESS.[9]

III. RESULTS AND DISCUSSION

A. Heat of Vaporization, ΔH_{vap}, of Water. To assess and develop appropriate EFP2 parameters, well-developed EFP1 and TIP5P parameters for water in GAMESS[9] were adopted. As indicated in the Computational Details, EFP1-MD and TIP5P-MD simulations with three different box sizes of 12.3, 15.0, and 20.0 Å were initially performed, which constitute 62, 113, and 267 explicit waters, respectively. The corresponding cubic boxes are shown Figure 1. The computed ΔH_{vap}(298 K) values by the EFP1 and TIP5P production runs converged in ∼10 ps, but the simulations continued for additional 40 ps. Moreover, the resulting ΔH_{vap}(298 K) is nearly independent of the box size, indicating that the model with 62 solvent molecules is sufficient to represent bulk water. (See Table 1)

The generations of EFP2 parameters were performed with three different theories of HF/6-31++G(2d,2p), HF/6-311+G-(2d,2p), and HF/6-311++G(3df,2p) to study the basis set effects using the standard procedure of GAMESS. After that, MD simulations with the three different parameters were performed with the box size of 12.3 Å. The computed ΔH_{vap}(298 K) values of water by EFP2 are listed in Table 1 along with those of EFP1 and TIP5P. As compared with the experimental ΔH_{vap}(298 K) of water, that is, 10.51 kcal/mol, both TIP5P and EFP1 yielded accurate predictions of 10.38 and 10.37 kcal/mol, respectively. The predicted values by the

dx.doi.org/10.1021/jp500365z | J. Phys. Chem. B 2014, 118, 4876−4882

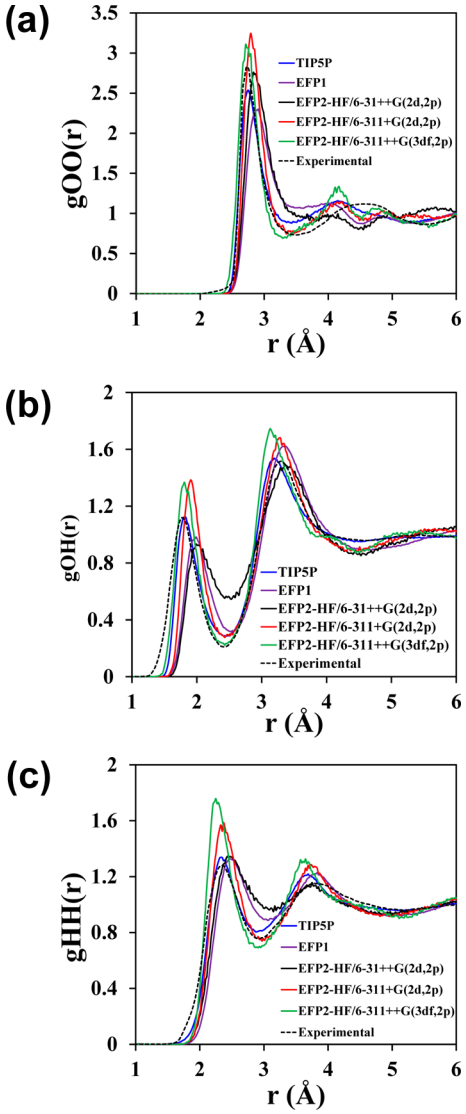

Figure 2. Radial distribution functions (RDFs)of (a) gOO(r), (b) gOH(r), and (c) gHH(r) as obtained by various water parameters.

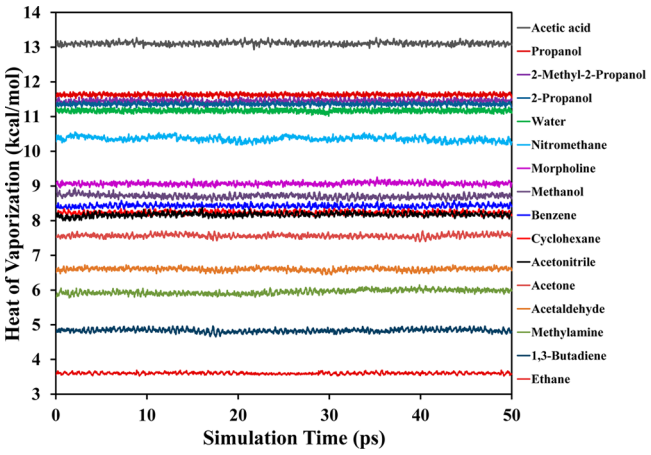

Figure 3. Time evolutions of the heats of vaporization (ΔH_{vap}) of 16 different molecules. All MD simulations were done with EFP2-HF/6-31++G(2d,2p) parameters.

three EFP2 parameters are slightly higher than that of EFP1. However, it should be emphasized that all of the EFP2 parameters are generated by a routine procedure without any experimental data. The EFP2 by HF/6-31++G(2d,2p) theory yielded 11.13 kcal/mol, which is the best agreement with experiment among the three EFP2 parameters. It appears that the agreements with experiment become worse with the increase in basis set size. This may be attributed to the overestimations of intermolecular interactions during MD simulations with larger basis set.

Radial distribution functions (RDFs), $g(r)$, were generated and presented in Figure 2 to study the characters of these EFP2 parameters in detail. The oxygen−oxygen, oxygen−hydrogen, and hydrogen−hydrogen distance distributions of various parameters with experiment are shown in Figure 2a−c, respectively. The peak heights of first peaks in the three figures by HF/6-311+G(2d,2p) and HF/6-311++G(3df,2p) appear to be higher than those of the other parameters and experiment, which may explain their overbinding characters. Although actual peak positions are not identical, the peak heights of TIP5P, EFP1, and EFP2-HF/6-31++G(2d,2p) parameters are more or less similar to each other, reflecting their consistency in predicting ΔH_{vap} predictions.

Damping of the electrostatic, polarization, and dispersion terms is very important to achieve correct asymptotic behavior and qualitative accuracy of the total EFP energies.[20] We tested the effects of damping parameters on the heat of vaporization of water. The combination of the Coulomb overlap-based damping, polarization Tang−Toennis style Gaussian damping, and dispersion overlap-based damping yielded the best agreement with the experimental value and was mainly adopted for the rest of our calculations. Other screening parameters show a slight overbinding character of the total EFP energies increasing the heat of vaporization by ∼0.06 kcal/mol. In addition, as compared with the valence virtual orbitals, canonical virtual orbitals overestimated the heat of vaporization by ∼0.3 kcal/mol, so the virtual valence orbitals for charge-transfer interaction were mainly utilized.

B. Heats of Vaporization, ΔH_{vap}, of Various Molecules.

To further generalize our observations of EFP2 performances, the ΔH_{vap} values of an additional 15 molecules were predicted by EFP2-MD. Because these 15 molecules exhibit a wide variation of ΔH_{vap}, they can form a good test set for EFP2 performance. The experimental and predicted ΔH_{vap} values with experimental densities, temperatures, and box sizes of each molecule for the simulations are presented in Table 2. It should be noted that temperatures of −88.63 and 128 °C were used for the simulations of ethane and morpholine, respectively. The convergences of $\Delta H_{vap}$of 16 molecules as simulated by EFP2-HF/6-31++G(2d,2p) are shown in Figure 3, in which it is seen that ΔH_{vap} values are quickly converged within 3 ps. Therefore, it is seen that the values are converged in ∼10 ps. The average computational times of our simulations were 10 ps/day on a moderate computer. In general, nearly all of our ΔH_{vap} predictions by EFP2 parameters are remarkably better than AMBER force fields,[7] considering that there is no experimental fitting procedure in the generation of EFP2 parameters. Among EFP2, as in the case of water, the EFP2-HF/6-31++G(2d,2p) parametrizations yielded the best predictions. Its MAD and RMSD are 0.34 and 0.44 kcal/mol, respectively. These deviations show that the prediction accuracy is <1 kcal/mol. Although further tests in various types of molecules are needed, it is generally seen that the EFP2 can be a very promising parametrization for the a priori predictions of ΔH_{vap}.

dx.doi.org/10.1021/jp500365z | J. Phys. Chem. B 2014, 118, 4876−4882

Table 3. Predicted Heats of Sublimation (ΔH_{sub})in kilocalories per mole for 16 Molecules[a]

molecule	$\Delta H_{fus}^{exp}(T_m)$[b]	ΔH_{sub}^{exp}[c]	ΔH_{sub}^{calc}[d]	$\Delta H_{sub}^{this\ work}$[d] HF/6-31++G(2d,2p)
water	1.44 (0.0)	11.95	14.84 (+2.89)	13.20 (+1.24)
ethane	0.67 (−183.5)	4.18	6.29 (+2.11)	4.27 (+0.09)
methylamine	1.47 (−93.3)	7.06	16.25 (+9.19)	6.99 (−0.07)
methanol	0.76 (−97.7)	9.60	11.70 (+2.10)	10.47 (+0.87)
acetonitrile	1.95 (−43.7)	9.82	8.56 (−1.26)	9.66 (−0.16)
acetaldehyde	0.41 (−30.1)	6.65	8.56 (+1.91)	7.76 (+1.11)
1,3-butadiene	1.91 (−108.8)	6.90	9.11 (+2.21)	5.77 (−1.13)
acetone	1.37 (−96.4)	8.84	9.97 (+1.13)	8.94 (+0.10)
acetic acid	2.80 (25.7)	15.13	15.38 (+0.25)	15.54 (+0.41)
propanol	1.28 (−124.2)	12.63	14.52 (+1.89)	13.67 (+1.04)
2-propanol	1.29 (−87.8)	12.14	14.52 (+2.38)	13.33 (+1.19)
nitromethane	2.32 (−28.2)	11.49	4.88 (−6.61)	12.14 (+0.65)
2-methyl-2-propanol	1.60 (26.0)	12.74	15.93 (+3.19)	13.58 (+0.84)
benzene	2.36 (5.7)	10.25	11.93 (+1.68)	9.81 (−0.44)
cyclohexane	0.64 (6.8)	8.53	11.93 (+3.40)	9.77 (+1.24)
morpholine	3.47 (−4.8)	12.34	18.20 (+5.86)	10.74 (−1.60)
MAD			**3.00**	**0.76**
RMSD			**3.75**	**0.90**

[a] ΔH_{fus} and ΔH_{sub} are in kilocalories per mole and melting temperature (T_m) is in degrees Celsius. The numbers in the parentheses of ΔH_{sub}s are deviations as compared with experiments. [b] Ref 26. [c] Sum of ΔH_{vap}^{exp} and ΔH_{fus}^{exp}. [d] Predicted by Charlton et al.'s MLRA method.[22] Current study with 1.185 scaling factor.

Table 4. Predicted Heats of Sublimation (ΔH_{sub}) for 30 Molecules by Using Scaling Factor 1.185[a]

molecule	ΔH_{vap}^{exp}[b]	ΔH_{sub}^{exp}[b]	ΔH_{sub}^{calc}
hydrogen cyanide	6.71	8.50	7.95 (−0.55)
trinitomethane	7.79	10.80	9.23 (−1.57)
carbon tetrachloride	8.05	9.27	9.54 (+0.27)
cyanogen fluoride	5.35	5.83	6.34 (+0.51)
carbonyl fluoride	4.78	5.54	5.66 (+0.12)
carbon tetraflouride	2.96	3.51	3.51 (0.00)
carbon monoxide	1.43	1.82	1.70 (−0.12)
chloroacetic acid	14.59	17.99	17.29 (−0.69)
3-chlorophenol	15.17	18.37	17.97 (−0.39)
4-chlorophenol	15.38	18.42	18.23 (−0.19)
2-nitrophenol	13.95	17.51	16.53 (−0.98)
propionamide	15.26	17.91	18.09 (+0.17)
acetone oxime	12.28	14.24	14.55 (+0.31)
N-methylacetamide	14.24	16.91	16.87 (−0.04)
ethyl carbamate	13.52	17.17	16.02 (−1.15)
propane	5.28	6.81	6.26 (−0.55)
1,3-diethylthiourea	22.21	25.80	26.32 (+0.53)
1,1,2-difluoro-1,2,2-trifluoroethane	6.76	7.86	8.01 (+0.15)
1,2-difluoro-1,1,2,2-tetrachloroethane	8.31	8.69	9.85 (+1.16)
hexachloroethane	12.83	14.09	15.20 (+1.11)
hexafluoroethane	4.13	6.21	4.90 (−1.31)
cyanogen	5.85	7.74	6.93 (−0.80)
acetylene	4.01	5.21	4.75 (−0.45)
tricosane	28.78	35.06	34.11 (−0.96)
1-methylfluorene	18.44	21.78	21.85 (+0.07)
9-methylfluorene	16.86	19.99	19.98 (−0.01)
benzil	16.53	19.78	19.59 (−0.19)
phenanthrene	18.80	220.9	22.27 (+0.18)
anthracene	18.75	23.00	22.22 (−0.78)
MAD			**0.53**
RMSD			**0.68**

[a] ΔH_{vap} and ΔH_{sub} are in kilocalories per mole. The numbers in parentheses of ΔH_{sub} are deviations as compared with experiments. [b] Ref 26.

dx.doi.org/10.1021/jp500365z | J. Phys. Chem. B 2014, 118, 4876−4882

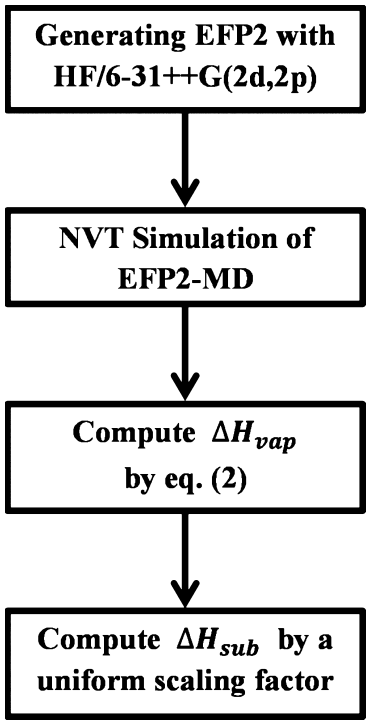

Figure 4. Overall computational procedure for ΔH_{vap} and ΔH_{sub}.

C. Heat of Sublimation, ΔH_{sub}. ΔH_{sub} is a simple sum of ΔH_{vap} and heat of fusion (ΔH_{fus}) at a same temperature (25 °C in most cases). Although most of ΔH_{vap} were measured experimentally at 25 °C, all ΔH_{fus} measurements were carried out at its melting point. Therefore, (1) the ΔH_{fus}value at the melting point and (2) the heat-capacity correction from the melting point to 25 °C are necessary. However, the heat-capacity correction term is known to be relatively small and disregarded.[21] The direct prediction of ΔH_{fus} is not so straightforward because it requires a clear understanding of solid-phase structure. To make matters worse, polymorph is occasionally present in certain molecules. Thus, the direct calculation of ΔH_{fus} is not a practical approach. Because it is usually the case that the magnitude of ΔH_{fus} is much smaller than that of ΔH_{vap}, one can develop a fitting procedure for ΔH_{sub} on the basis of ΔH_{vap} predictions. By introducing a uniform scaling factor, s, the experimental ΔH_{sub} of 16 molecules was fitted against predicted ΔH_{vap} by EFP2-HF/6-31++G(2d,2p) parameters. The optimum scale factor, s, was determined to be 1.185 by minimizing the residual

$$\Delta = \sum_{i}^{\text{all}} (\Delta H_{\text{sub},i} - s \cdot \Delta H_{\text{vap},i})^2 \quad (3)$$

The predicted ΔH_{sub} values by a scaling factor are presented in Table 3 along with the values, as predicted by a multilinear regression analysis (MLRA).[22] Our maximum deviation of predicted ΔH_{sub} is 1.60 kcal/mol (morpholine) as compared with the experiment. Consequently, the MAD and RMSD of our procedure for 16 molecules are 0.76 and 0.90 kcal/mol, respectively. The MLRA method also yielded reasonable predictions, although its overall accuracy is worse than ours. To make matters worse, the error of MLRA can be as big as 9.19 kcal/mol in the case of methylamine, showing its unpredictable deviations. To validate our simple procedure for the prediction of ΔH_{sub} on the basis of theoretical ΔH_{vap}, the same scale factor was tested between experimental ΔH_{sub} and ΔH_{vap}, and the results are presented in Table 4. An additional 30 molecules were tested in which the ΔH_{sub} values are predicted by experimental ΔH_{vap} with our scaling factor. As shown in Table 4, the overall MAD and RMSD for 30 molecules are 0.53 and 0.68, respectively, validating our simple procedure. In short, we demonstrated that high-accuracy predictions of both ΔH_{vap} and ΔH_{sub} can be feasible by combining EFP2-MD simulations and a simple fitting procedure. Our overall prediction procedure for ΔH_{vap} and ΔH_{sub} is summarized in Figure 4. The whole procedure starts from the generations of EFP2 parameters, for which the HF/6-31++G(2d,2p) is recommended. Subsequent, EFP2-MD simulation is done, which yields the ΔH_{vap} by eq 2. The ΔH_{sub} is finally obtained by a simple scale procedure of predicted ΔH_{vap}.

IV. CONCLUSIONS

New theoretical procedures were proposed for the accurate predictions of ΔH_{vap} and ΔH_{sub} and tested with 16 different molecules. Our procedures are composed of MD simulations with EFP2 parameters and a simple fitting by a uniform scaling factor. Because EFP2 is fully ab initio parameters, it is emphasized that no experimental information is needed in our procedure. The EFP2-MD simulations with the particular HF/6-31++G(2d,2p) parameters exhibited the best agreements with experiments in the predictions of ΔH_{vap}. The MAD and RMSD of ΔH_{vap} predictions are 0.34 and 0.44 kcal/mol, respectively, indicating that a chemical accuracy can be achieved. By introducing a uniform scaling factor of 1.185 on the basis of predicted ΔH_{vap}, highly accurate ΔH_{sub} predictions were also achieved, yielding MAD and RMSD to be 0.76 and 0.90 kcal/mol, respectively. Because EFP2-MD simulations do not utilize any ab initio computations during MD simulation and the convergences of the intermolecular potential energies are fast, the computational effort of EFP2-MD simulations is minimal. We believe that our current procedure can be useful in the developments of new materials, where the availability of experimental data is limited.

AUTHOR INFORMATION

Corresponding Author

*E-mail: cchoi@knu.ac.kr. Tel:+82-53-950-5332. Fax:+82-53-950-6330.

Notes

The authors declare no competing financial interest.

ACKNOWLEDGMENTS

This work was supported by the Agency for Defense Development (ADD) and by the National Research Foundation of Korea (NRF) grant funded by the Korea government (MEST) (No. 2007-0056341and No. 2012-0004812).

REFERENCES

(1) Fried, L. E. *CHEETAH: a Fast Thermochemical Code for Detonation*; United States Department of Energy: Washington, DC, 1993

(2) Sućeska, M. Calculation of Detonation Parameters by EXPLO5 Computer Program. *Mater. Sci. Forum* **2004**, *465−466*, 325−330.

(3) Pankow, J. F.; Asher, W. E. SIMPOL.1: a Simple Group Contribution Method for Predicting Vapor Pressures and Enthalpies

of Vaporization of Multifunctional Organic Compounds. *Atmos. Chem. Phys.* **2008**, *8*, 2773−2796.
(4) Dalmazzone, D.; Salmon, A.; Guella, S. A Second Order Group Contribution Method for the Prediction of Critical Temperatures and Enthalpies of Vaporization of Organic Compounds. *Fluid Phase Equilib.* **2006**, *242*, 29−42.
(5) Politzer, P.; Ma, Y.; Lane, P.; Concha, M. C. Computational Prediction of Standard Gas, Liquid, and Solid-Phase Heats of Formation and Heats of Vaporization and Sublimation. *Int. J. Quantum Chem.* **2005**, *105*, 341−347.
(6) Wang, J.; Hou, T. Application of Molecular Dynamics Simulations in Molecular Property Prediction. 1. Density and Heat of Vaporization. *J. Chem. Theory Comput.* **2011**, *7*, 2151−2165.
(7) Mackerell, A. D.; Shim, J. H.; Anisimov, V. M. Re-Evaluation of the Reported Experimental Values of the Heat of Vaporization of N-Methylacetamide. *J. Chem. Theory Comput.* **2008**, *4*, 1307−1312.
(8) Gordon, M. S.; Slipchenko, L.; Li, H.; Jensen, J. H. The Effective Fragment Potential: a General Method for Predicting Intermolecular Interactions. *Ann. Rep. Comput. Chem.* **2007**, *3*, 177−193.
(9) Schmidt, M. W.; Baldridge, K. K.; Boatz, J. A.; Elbert, S. T.; Gordon, M. S.; Jensen, J. H.; Koseki, S.; Matsunaga, N.; Nguyen, K. A.; Su, S.; et al. General Atomic and Molecular Electronic Structure System. *J. Comput. Chem.* **1993**, *14*, 1347−1363.
(10) Gordon, M. S.; Fedorov, D. G.; Pruitt, S. R.; Slipchenko, L. V. Fragmentation Methods: a Route to Accurate Calculations on Large Systems. *Chem. Rev.* **2012**, *112*, 632−672.
(11) Choi, C. H.; Re, S.; Feig, M.; Sugita, Y. Chemical Physics Letters. *Chem. Phys. Lett.* **2012**, *539*−*540*, 218−221.
(12) Car, R.; Parrinello, M. Unified Approach for Molecular Dynamics and Density-Functional Theory. *Phys. Rev. Lett.* **1985**, *55*, 2471−2474.
(13) Choi, C. H.; Re, S.; Rashid, M. H. O.; Li, H.; Feig, M.; Sugita, Y. Solvent Electronic Polarization Effects on Na +−Na +and Cl −−Cl −Pair Associations in Aqueous Solution. *J. Phys. Chem. B* **2013**, *117*, 9273−9279.
(14) Uddin, N.; Choi, T. H.; Choi, C. H. Direct Absolute PKa Predictions and Proton Transfer Mechanisms of Small Molecules in Aqueous Solution by QM/MM-MD. *J. Phys. Chem. B* **2013**, *117*, 6269−6275.
(15) Ghosh, M. K.; Uddin, N.; Choi, C. H. Hydrophobic and Hydrophilic Associations of a Methanol Pair in Aqueous Solution. *J. Phys. Chem. B* **2012**, *116*, 14254−14260.
(16) Ghosh, M. K.; Re, S.; Feig, M.; Sugita, Y.; Choi, C. H. Interionic Hydration Structures of NaCl in Aqueous Solution: a Combined Study of Quantum Mechanical Cluster Calculations and QM/EFP-MD Simulations. *J. Phys. Chem. B* **2013**, *117*, 289−295.
(17) Mahoney, M. W.; Jorgensen, W. L. A Five-Site Model for Liquid Water and the Reproduction of the Density Anomaly by Rigid, Nonpolarizable Potential Functions. *J. Chem. Phys.* **2000**, *112*, 8910−8922.
(18) Nosé, S. A Unified Formulation of the Constant Temperature Molecular Dynamics Methods. *J. Chem. Phys.* **1984**, *81*, 511−519.
(19) Hoover, W. Canonical Dynamics: Equilibrium Phase-Space Distributions. *Phys. Rev. A* **1985**, *31*, 1695−1697.
(20) Slipchenko, L. V.; Gordon, M. S. Damping Functions in the Effective Fragment Potential Method. *Mol. Phys.* **2009**, *107*, 999−1016.
(21) *Molecular Structure and Energetics: Physical Measurements*; Wiley-VCH: Deerfield Beach, FL, 1987; Vol. 2.
(22) Charlton, M. H.; Docherty, R.; Hutchings, M. G. Quantitative Structure−Sublimation Enthalpy Relationship Studied by Neural Networks, Theoretical Crystal Packing Calculations and Multilinear Regression Analysis. *J. Chem. Soc., Perkin Trans. 2* **1995**, 2023−2030.
(23) *CRC Handbook of Chemistry and Physics*, 86th ed.; Lide, D. R., Ed.; CRC Press: Boca Raton, FL, 2005.
(24) Majer, V.; Svoboda, V. *Enthalpies of Vaporization of Organic Compounds: A Critical Review and Data Compilation*; Blackwell Scientific: Oxford, U. K., 1985.
(25) Wiberg, K. B.; Crocker, L. S.; Morgan, K. M. Thermochemical Studies of Carbonyl Compounds. 5. Enthalpies of Reduction of Carbonyl Groups. *J. Am. Chem. Soc.* **1991**, *113*, 3447−3450.
(26) Acree, W., Jr.; Chickos, J. S. Phase Transition Enthalpy Measurements of Organic and Organometallic Compounds. Sublimation, Vaporization and Fusion Enthalpies from 1880 to 2010. *J. Phys. Chem. Ref. Data* **2010**, *39*, 043101.